J|A|C|S
ARTICLES
Published on Web 04/06/2007

Gas Sensing Mechanism in Chemiresistive Cobalt and Metal-Free Phthalocyanine Thin Films

Forest I. Bohrer,[†] Amos Sharoni,[‡] Corneliu Colesniuc,[‡] Jeongwon Park,[#] Ivan K. Schuller,*[,‡] Andrew C. Kummel,*[,†] and William C. Trogler*[,†]

Contribution from the Department of Chemistry and Biochemistry, Materials Science and Engineering Program, and Department of Physics, University of California, San Diego, 9500 Gilman Drive, La Jolla, California 92093

Received December 13, 2006; E-mail: ischuller@ucsd.edu; akummel@ucsd.edu; wtrogler@ucsd.edu

Abstract: The gas sensing behaviors of cobalt phthalocyanine (CoPc) and metal-free phthalocyanine (H_2-Pc) thin films were investigated with respect to analyte basicity. Chemiresistive sensors were fabricated by deposition of 50 nm thick films on interdigitated gold electrodes via organic molecular beam epitaxy (OMBE). Time-dependent current responses of the films were measured at constant voltage during exposure to analyte vapor doses. The analytes spanned a range of electron donor and hydrogen-bonding strengths. It was found that, when the analyte exceeded a critical base strength, the device responses for CoPc correlated with Lewis basicity, and device responses for H_2Pc correlated with hydrogen-bond basicity. This suggests that the analyte−phthalocyanine interaction is dominated by binding to the central cavity of the phthalocyanine with analyte coordination strength governing CoPc sensor responses and analyte hydrogen-bonding ability governing H_2Pc sensor responses. The interactions between the phthalocyanine films and analytes were found to follow first-order kinetics. The influence of O_2 on the film response was found to significantly affect sensor response and recovery. The increase of resistance generally observed for analyte binding can be attributed to hole destruction in the semiconductor film by oxygen displacement, as well as hole trapping by electron donor ligands.

Introduction

Phthalocyanines (Pcs), both metalated (MPcs) and metal-free (H_2Pc), are organic semiconductors that have been identified as promising candidates for gas sensors.[1,6,7] They are chemically sensitive to reactive gases and show potential for chemical selectivity via manipulation of the metal center and substitution of functional groups on the organic ring.[1−5] Conductivity in Pc films is influenced strongly by atmospheric "dopants", primarily O_2.[8] It has been reported that Pcs are insulating in a dark high vacuum environment.[9] However, when Pc thin films are exposed to O_2, the films become doped and the conductivity increases dramatically. This air-induced conductivity has been attributed to different mechanisms. For polycrystalline films, it is assumed that O_2 absorbs only at the air/MPc interface and at grain boundaries because the MPc crystal structure is very tight and unaffected by exposure to air.[2−4] It has been reported that the formation of charge-transfer complexes by coordination of O_2 to MPc metal centers at the air/phthalocyanine interface leads to the formation of oxidized MPc^+ and O_2^- species and injection of hole charge carriers into the bulk solid.[8,10,11] The presence of the superoxide adduct of CoPc has been detected in several electron paramagnetic resonance (EPR) studies.[12,13] There is also evidence that weaker O_2 adsorption may occur on the four *meso*-nitrogens of free base H_2Pc, leading to conductivity increases that are not as large as those for the MPcs.[2−4] As a surface dopant, O_2 occupies only a fraction of the binding sites on the film;[8] therefore, interactions with analyte vapors in air could result in two different mechanisms of analyte binding (Scheme 1). Analytes could either bind to open surface metal coordination sites or compete with O_2 for occupied metal surface sites. There is the additional possibility of weak binding (physisorption) to the organic region of the Pc molecule for noncoordinating analytes, which may be governed by weak hydrophobic and possibly charge-transfer interactions.

Previous mechanistic studies of solid-state gas sensors have been studied in the context of both conduction mechanisms and

[†] Department of Chemistry and Biochemistry.
[#] Materials Science and Engineering Program.
[‡] Department of Physics.

(1) Snow, A. W.; Barger, W. R. Phthalocyanine Films in Chemical Sensors. In *Phthalocyanines: Properties and Applications*; Lever, A. B. P., Ed.; John Wiley and Sons: New York, 1989; Vol. 1, p 341.
(2) Wright, J. D. *Prog. Surf. Sci.* **1989**, *31*, 1−60.
(3) Guillaud, G.; Simon, J.; Germain, J. *Coord. Chem. Rev.* **1998**, *178*, 1433−1484.
(4) Gould, R. D. *Coord. Chem. Rev.* **1996**, *156*, 237−274.
(5) Albert, K. J.; Lewis, N. S.; Schauer, C. L.; Sotzing, G. A.; Stitzel, S. E.; Vaid, T. P.; Walt, D. R. *Chem. Rev.* **2000**, *100*, 2595−2626.
(6) Eley, D. *Nature* **1948**, *162*, 819.
(7) Wilson, A.; Collins, R. A. *Sens. Actuators* **1987**, *12*, 389−403.
(8) Kerp, H. R.; Westerdui, K. T.; van Veen, A. T.; van Faassen, E. E. *J. Mater. Res.* **2001**, *16*, 503−511.
(9) de Haan, A.; Debliquy, M.; Decroly, A. *Sens. Actuators B* **1999**, *57*, 69−74.
(10) Simon, J.; Andre, J. J. *Molecular Semiconductors*; Springer-Verlag: Berlin, 1985; pp 73−149.
(11) Ho, K. C.; Tsou, Y. H. *Sens. Actuators B* **2001**, *77*, 253−259.
(12) Zwart, J.; Van Wolput, J. H. M. C. *J. Mol. Catal.* **1979**, *5*, 51−64.
(13) Yahiro, H.; Naka, T.; Kuramoto, J.; Kurohagi, K.; Okada, G.; Shiotani, M. *Microporous Mesoporous Mater.* **2005**, *79*, 291−297.

10.1021/ja0689379 CCC: $37.00

Scheme 1. Chemisorption Model of CoPc Interaction with Oxygen and Coordinating Analytes L: For Noncoordinating Analytes, Rapid Reversible Adsorption on the Pc Rings is Attributed to the Weak Sensor Responses Observed

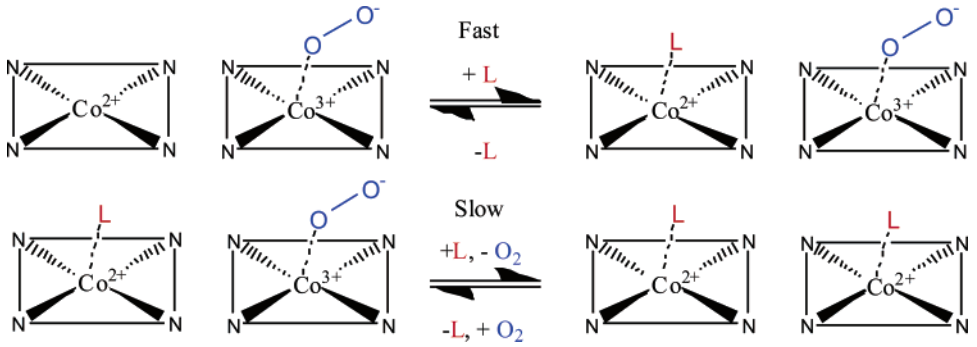

molecular interactions. The responses of metal oxide gas sensors, primarily SnO_2, have been widely explored with respect to surface adsorption, chemical reaction, and resulting conductivity changes.[14,15] These sensors are operated at elevated temperatures (100−500 °C), and reactive oxygen species (O_2^-, O^-, and O^{2-}) are present at the surface of the SnO_2 grains.[16] These oxygen species engage in redox reactions with analytes such as water, carbon monoxide, and methane. The subsequent changes in grain surface charge alters the film conductivity, which has been rationalized using a band-bending model.[17]

Organic thin film sensors rely on weak intermolecular interactions rather than redox chemistry. Organic coatings encompass a wide variety of structures, including molecular crystals, liquid crystals, molecular cages, nanotubes, and polymers.[18] A variety of detection methods have been applied to organic sensors: these include spectroscopic detection,[19,20] surface acoustic wave (SAW) technology,[21] and chemiresistive devices.[22] Linear solvation energy relationships (LSER) have been used to understand analyte interactions in thin film polymer sensors; this model incorporates such molecular properties as dispersion (van der Waals forces and π stacking), polarizability, dipolarity, and hydrogen-bond basicity and acidity.[23,24] These intermolecular interactions have been probed directly via FT-IR spectroscopy.[25] Resistive sensing studies with p-type Pc thin films have focused primarily on their interaction with oxidizing gases, such as ozone and NO_X.[26−30] Pc films are easily oxidized by NO_X, forming charge-transfer complexes, which inject holes and increase film currents. The interaction of Pcs with reducing gases, such as NH_3, has the opposite effect. Decreased current upon analyte binding to these films has been attributed to electron donation from the reducing gas to trap charge carriers.[31] Attempts have been made to relate MPc sensing to band theory.[32−34] However, the magnitude of sensor response has not been quantitatively correlated with molecular properties of the analyte.

One postulate is that metal−analyte coordination strength should primarily govern analyte binding and therefore the response of CoPc chemiresistive sensors to non-oxidizing gases. Similarly, for H_2Pc chemiresistive sensors, the hydrogen bonding of analyte to the two interior NH protons should primarily govern sensor responses. In order to test whether the anticipated molecular interactions between analytes and surface Pc molecules dominated the sensor response, we measured the CoPc and H_2Pc sensor responses to analytes with a wide range of established Lewis basicities and hydrogen-bond acceptor abilities.

Much research has been devoted to developing empirical scales of electron donation and basicity in molecules. Kamlet and Taft established the pK_{HB} scale of hydrogen-bond basicity using log K values ($dm^3 \cdot mol^{-1}$) of complexation of bases with 4-fluorophenol in CCl_4.[35,36] This scale has been expanded using a variety of reference acids to create the extensive β_2^H scale of hydrogen-bond basicities used in the present study.[37] Gutmann quantified Lewis basicities of aprotic electron donors as the molecular donor number (DN).[38,39] The donor number is defined as the enthalpy ($kcal \cdot mol^{-1}$) of formation of a 1:1 adduct of a Lewis base to the Lewis acid $SbCl_5$. Unfortunately, there are several notable inaccuracies in this scale.[40] Maria and Gal improved on the DN concept by establishing the $-\Delta H^o_{BF_3}$ scale, a rigorous, calorimetrically determined enthalpy scale ($kJ \cdot mol^{-1}$) of adducts with the Lewis acid BF_3.[41] This was used in the present study as an experimental measure of electron pair donor ability, with the possible shortcoming that the softer Lewis acid

(14) Lundstrom, I. *Sens. Actuators B* **1996**, *35*, 11−19.
(15) Fleischer, M.; Meixner, H. *J. Vac. Sci. Technol. A* **1999**, *17*, 1866−1872.
(16) Nakata, S.; Okunishi, H. *Appl. Surf. Sci.* **2005**, *240*, 366−374.
(17) Barsan, N.; Schweizer-Berberich, M.; Gopel, W. *Fresenius J. Anal. Chem.* **1999**, *365*, 287−304.
(18) Gopel, W. *Sens. Actuators B* **1995**, *24*−*25*, 17−32.
(19) Dunbar, A. D. F.; Richardson, T. H.; McNaughton, A. J.; Hutchinson, J.; Hunter, C. A. *J. Phys. Chem. B* **2006**, *110*, 16646−16651.
(20) Armstrong, N. R. *J. Porphyrins Phthalocyanines* **2000**, *4*, 414−417.
(21) Nieuwenhuizen, M. S.; Nederlof, A. J.; Barendsz, A. W. *Anal. Chem.* **1988**, *60*, 230−235.
(22) Bekyarova, E.; Davis, M.; Burch, T.; Itkis, M. E.; Zhao, B.; Sunshine, S.; Haddon, R. C. *J. Phys. Chem. B* **2004**, *108*, 19717−19720.
(23) Grate, J. W.; Abraham, M. H. *Sens. Actuators B* **1991**, *3*, 85−111.
(24) Grate, J. W. *Chem. Rev.* **2000**, *100*, 2627−2648.
(25) Hierlemann, A.; Ricco, A. J.; Bodenhofer, K.; Gopel, W. *Anal. Chem.* **1999**, *71*, 3022−3035.
(26) Lee, Y. L.; Hsiao, C. Y.; Chang, C. H.; Yang, Y. M. *Sens. Actuators B* **2003**, *94*, 169−175.
(27) Liu, C. J.; Hsieh, J. C.; Ju, Y. H. *J. Vac. Sci. Technol. A* **1996**, *14*, 753−756.
(28) Zhou, Q.; Gould, R. D. *Thin Solid Films* **1998**, *317*, 436−439.
(29) Sadaoka, Y.; Jones, T. A.; Gopel, W. *Sens. Actuators B* **1990**, 148−153.
(30) Germain, J. P.; Pauly, A.; Maleysson, C.; Blanc, J. P.; Schollhorn, B. *Thin Solid Films* **1998**, *333*, 235−239.
(31) Schollhorn, B.; Germain, J. P.; Pauly, A.; Maleysson, C.; Blanc, J. P. *Thin Solid Films* **1998**, *326*, 245−250.
(32) Orti, E.; Bredas, J. L. *J. Am. Chem. Soc.* **1992**, *114*, 8669−8675.
(33) Shihub, S. I.; Gould, R. D. *Thin Solid Films* **1995**, *254*, 187−193.
(34) Schlettwein, D.; Hesse, K.; Gruhn, N. E.; Lee, P. A.; Nebesny, K. W.; Armstrong, N. R. *J. Phys. Chem. B* **2001**, *105*, 4791−4800.
(35) Taft, R. W.; Gurka, D.; Joris, L.; Schleyer, P. v. R.; Rakshys, J. W. *J. Am. Chem. Soc.* **1969**, *91*, 4801−4808.
(36) Kamlet, M. J.; Taft, R. W. *J. Am. Chem. Soc.* **1976**, *98*, 377−383.
(37) Abraham, M. H.; Grellier, P. L.; Prior, D. V.; Morris, J. J.; Taylor, P. J. *J. Chem. Soc., Perkins Trans. 2* **1990**, 521−529.
(38) Gutmann, V. *Electrochim. Acta* **1976**, *21*, 661−670.
(39) Gutmann, V. *Coord. Chem. Rev.* **1976**, *18*, 225−255.
(40) Gritzner, G. *J. Mol. Liquids* **1997**, *73*, 487−500.
(41) Maria, P. C.; Gal, J. F. *J. Phys. Chem.* **1985**, *89*, 1296−1304.

character of Co(II) as compared to boron(III) would require using donor ligands of similar hard/soft character.[42]

Experimental Section

1. Electrode Fabrication. Interdigitated electrodes (IDEs) were prepared by standard photolithography and lift-off processing on thermally grown SiO_2 (thickness of 1 μm) on (100) Si substrates. The electrodes consist of 45 pairs of gold fingers, spaced 5 μm apart, with an electrode width of 2 mm. The electrodes were deposited by electron beam evaporation. An adhesion layer of 5 nm Ti was applied first, followed by 45 nm of Au for a total electrode thickness of 50 nm. Six pairs of electrodes were grown on each substrate to verify sensor reproducibility and increase yield.

2. Thin Film Deposition. CoPc (Aldrich, 97%) and H_2Pc (Aldrich, 98%) were purified via multiple zone sublimations at 400 °C and 10^{-5} Torr. Films of a thickness of 50 nm were deposited on six IDEs per substrate by organic molecular beam epitaxy (OMBE) in a UHV chamber with a base pressure of 2×10^{-10} Torr. The deposition rate of the Pc films ranged from 0.2 to 0.5 Å/s, and the deposition pressure was 5×10^{-9} Torr. Film growth rate and thickness were monitored with a quartz crystal microbalance (QCM). The IDEs were mounted on a temperature-controlled stage monitored with two thermocouples. Substrate temperature during deposition was held constant at 25 ± 1 °C. After deposition, the devices were stored under vacuum at 10 mTorr or less until use. The thickness of the films was confirmed by low-angle XRD measurements performed on a Rigaku RU-200B diffractometer using Cu Kα radiation.[43]

3. Device Measurements. Chemical responses of CoPc and H_2Pc IDE sensors were measured inside a test chamber of stainless steel coated with a passivating layer of SiO_2. The internal volume of the chamber was 15 cm^3. The IDEs were placed in ceramic chip mounts purchased from Spectrum Semiconductor Technologies L.L.C. Gold leads were wirebonded from the IDEs to the mounts. Two sensor arrays could be placed in the chamber at a time for simultaneous mounting of six CoPc and six H_2Pc IDE devices. Contacts were made to the chip mounts via electrical feedthroughs in the top of the test chamber. The internal temperature of the chamber was monitored by a thermocouple and maintained at 50 ± 0.1 °C by coolant lines connected to a Haake F8 constant temperature bath. A Keithley 6517/6521 multichannel electrometer was used both as voltage source and ammeter, enabling 10 sensors to be tested simultaneously. The devices were placed in the chamber in the absence of light for 24 h before being tested to ensure the decay of residual photoconductivity. Analyte vapors were introduced into the sensor chamber by a system of bubblers and mass flow controllers. Zero grade air (<0.1 ppm of NO_X and SO_X and <5 ppm H_2O) and ultrahigh purity (UHP) nitrogen were used as carrier gases. A constant flow rate of 500 sccm (standard cm^3 per minute) was applied during the dosing/purging cycle. Analytes were introduced into the flow by bubblers immersed in a Haake F8 constant temperature bath. Mass flow controllers (MKS Instruments, Inc. 1479A, 10 and 1000 sccm) were used in conjunction with the bubblers and a four-way valve to saturate the carrier gas with a known concentration of analyte before introduction into the sensor chamber. Solenoid valves were placed before and after each bubbler to prevent cross contamination of analytes. A Labview VI program was used to control all instruments and record data.

Analytes were chosen to span both β_2^H and $-\Delta H^o_{BF_3}$ scales, including dichloromethane, nitromethane, acetonitrile, 2-butanone, di-*n*-butyl ether, trimethyl phosphate, water, isophorone, dimethyl methylphosphonate (DMMP, a neurotoxin simulant),[44] dimethyl sulfoxide (DMSO), *N*,*N*-dimethylformamide (DMF), and triethylamine, in order of increasing $-\Delta H^o_{BF_3}$ values. All analytes were of analytical purity (99.5+%) and dried over 4 Å molecular sieves (Fisher). All analytes were purchased from Aldrich except isophorone (Acros) and DMMP (Strem). Table 1 lists analytes and their β_2^H and $-\Delta H^o_{BF_3}$ values. Analyte doses were delivered as saturated vapors at specific flow rates and then diluted to 500 sccm. The ratio of vapor from the bubbler to dilution gas was controlled with mass flow controllers. Vapor pressure data[45] were used with the Clausius−Clapeyron equation to calculate the concentration of each dose in parts per million (ppm). Dichloromethane, nitromethane, acetonitrile, and 2-butanone were dosed at 225, 450, 675, and 900 ppm. Di-*n*-butyl ether, trimethyl phosphate, water, isophorone, DMMP, DMSO, DMF, and triethylamine were dosed at 90, 135, 180, and 225 ppm. Before dosing, the devices were annealed at 70 °C in order to drive off any adsorbed molecules and achieve a stable baseline current.

Table 1. Lewis Basicities ($-\Delta H^o_{BF_3}$)[39] and Hydrogen-Bond Basicities (β_2^H)[35] for Analytes Studied

analyte	$-\Delta H^o_{BF_3}$ (kJ·mol^{-1})	β_2^H
dichloromethane	10.0	0.05
nitromethane	37.63	0.25
acetonitrile	60.39	0.31
2-butanone	76.07	0.48
di-*n*-butyl ether	78.57	0.46
trimethyl phosphate	84.79	0.76
water		0.38
isophorone	90.56	0.52
DMMP[a]		0.81
DMSO	105.34	0.78
DMF	110.49	0.66
triethylamine	135.87	0.67

[a] The β_2^H value for DMMP was estimated from experimental values for dimethyl ethylphosphonate and diethyl methylphosphonate.

Results and Discussion

1. Film Characterization. Surface morphology was measured by atomic force microscopy (AFM) using a Nanoscope IV scanning microscope in tapping mode and a Veeco 200 kHz probe. The films had a granular structure with ellipsoidal grains of approximately 50 nm diameter on the long axis and an rms roughness of 5 nm. XRD revealed the films deposited at 25 °C to be textured α phase.[43] *I*−*V* measurements were recorded in the test chamber at 5 degree increments in a range from 5 to 50 °C. Voltage was stepped from 10 to −10 V in 0.1 V increments. The devices were allowed to equilibrate at each temperature and voltage. All devices reported had good ohmic behavior at low voltages. Space charge limited conductivity (SCLC) was found to occur, in general, above 5 V. Miller and co-workers showed that operation of MPc IDEs in the SCLC regime removes influence of the electrode/MPc interface on the chemical sensing.[46] Device responses were measured at 8 V, which is well within the SCLC regime. At 8 V, the CoPc devices had a base current on the order of 1 μA, while the H_2Pc devices had a base current of approximately 1 nA.

Figure 1 shows the CoPc sensor response to a 40 min dose of DMMP (78 ppm) using zero grade air as the carrier gas. In many studies, 40 min is sufficient time at room temperature to reach the saturation region of the sensor response.[9,11,28,47−49] This figure illustrates that there are two temporal components

(42) Pearson, R. G. *Hard and Soft Acids and Bases*; Dowden, Hutchinson, and Ross: Stroudsville, PA, 1973.
(43) Miller, C. W.; Sharoni, A.; Liu, G.; Colesniuc, C. N.; Fruhberger, B.; Schuller, I. K. *Phys. Rev. B* **2005**, *72*, 104113.
(44) Marrs, T. C. *Pharmacol. Ther.* **1993**, *58*, 51−66.
(45) Lide, D. R., Frederikse, H. P. R., Eds. *CRC Handbook of Chemistry and Physics*, 74th ed.; CRC Press: Ann Arbor, MI, 1993; Section 9.
(46) Miller, K. A.; Yang, R. D.; Hale, M. J.; Park, J.; Fruhberger, B.; Colesniuc, C. N.; Schuller, I. K.; Kummel, A. C.; Trogler, W. C. *J. Phys. Chem. B* **2006**, *110*, 361−366.

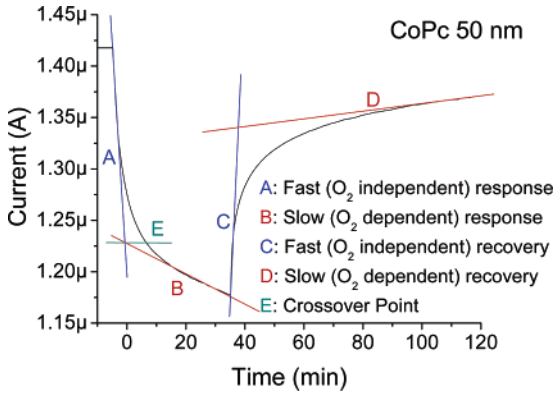

Figure 1. A 40 min DMMP pulse in air with both fast (oxygen-independent) and slow (oxygen-dependent) portions labeled. The crossover point is determined as the point where the response shifts from fast to slow, which occurs at ~5 min.

to sensor response and recovery. There is an initial fast region, which accounts for the largest change in the sensor current (A, C), followed by a slower saturation region (B, D). The fast response (A) is approximately equivalent to the fast recovery (C), while the slow saturation response (B) is approximately equivalent to the slow recovery (D). A mechanism involving O_2 binding to weak and strong sites has been previously suggested for NiPc sensors exposed to NO.[11] In our model, the fast portion of the response would correspond to binding of analyte at oxygen-free sites and the slow portion to competitive displacement of oxygen-bound sites (Scheme 1). This is supported by the vapor-phase O_2 dependence of the sensor responses (vide infra). At room temperature, the crossover point between the oxygen-independent (fast) and oxygen-dependent (slow) sensor response occurs near 5 min (E). In order to reduce recovery times, the primarily oxygen-independent response was examined by using 5 min doses at a temperature of 50 °C.

2. Sensor Response Kinetics. Responses of the CoPc and H_2Pc IDE sensors were determined from the time-dependent current plots of the films when dosed with analyte. The weaker analytes (dichloromethane through 2-butanone) were dosed with a 20% duty cycle (5 min doses with 20 min recovery times). The stronger analytes (di-*n*-butyl ether through triethylamine) were dosed with a 5% duty cycle (5 min doses with 90 min recovery). Raw data for both sensors are shown in Figure 2.

It can be seen qualitatively in Figure 2 that the changes in current of the films scale with analyte concentration. It should be noted that some oxygen-dependent effects are seen in the sensor recoveries from strong analytes (those above the critical threshold; vide infra). Thus we should consider the fast portion of the response and recovery *primarily* oxygen-independent, with some oxygen-dependent character. In order to quantitatively analyze the sensor responses, the percent current change was calculated for each dose, using eq 1

$$\%\ \text{current change} = [(I_0 - I_f)/I_0] \times 100 \qquad (1)$$

where I_0 is the current at the start of the dose and I_f is the current at the end of the 5 min dose. This value is designated as the sensor response. It can be seen in Figure 3 that CoPc sensor responses are linear with respect to analyte concentration (in general $R^2 \geq 0.97$), suggesting first-order analyte−film interaction kinetics. H_2Pc sensor responses are similarly linear. The slopes R_C (% ppm^{-1}) of the linear fits for each analyte increase with increasing sensor response and are used as device responses combining data from all doses.

First-order kinetics analysis as developed by Tongpool et al. was used to model the kinetics of gas−MPc sensor interactions.[50] The response curves appear to follow a first-order decay process; the reaction rate equation, r, is

$$r = -\mathrm{d[A]}/\mathrm{d}t = k[\mathrm{A}] \qquad (2)$$

with k as the sensor response rate constant and [A] as the concentration of species A.[51] By integration, this equation becomes

$$\ln[\mathrm{A}_t] = \ln[\mathrm{A}_0] - k(t - t_0) \qquad (3)$$

where $[A_0]$ is the initial concentration of A and $[A_t]$ is the concentration of A at time t. This may be adapted to the sensors by defining $[A_t]$ as $(I_t - I_f)$ where I_t is the current at time t and I_f is the final current of the dose. Consequently, if the plot of $\ln(I_t - I_f)$ versus t is linear, the reaction is first order and the slope of the line is $-k$. Figure 4 shows plots of $\ln(I_t - I_f)$ versus t for the strong analytes. Examination of these plots shows that the rates of sensing for all analytes are similar, with a range of $0.17\ \text{min}^{-1} \leq k \leq 0.45\ \text{min}^{-1}$. The H_2Pc sensor responses also obey first-order kinetics, with rate constants in the range of $0.15\ \text{min}^{-1} \leq k \leq 0.60\ \text{min}^{-1}$. These data suggest that sensor adsorption mechanisms are similar for all analytes.

3. CoPc Sensitivity. CoPc sensitivity was analyzed by correlating the slopes R_C (% ppm^{-1}, Figure 3) of all analytes to the $-\Delta H^o_{BF_3}$ scale. Figure 5 plots R_C versus $-\Delta H^o_{BF_3}$ for all analytes. It can be seen that above the threshold value of 73.7 kJ·mol^{-1} there is a strong linear dependence of sensor response with Lewis basicity. The sensor is relatively insensitive to analytes with $-\Delta H^o_{BF_3}$ values below this threshold, with small (<0.2%) and completely reversible sensor responses. There are two outliers to the observed correlation, DMSO and isophorone; however, these outliers can be attributed to inconsistencies within the $-\Delta H^o_{BF_3}$ scale. DMSO possesses a soft, electron-rich sulfur center that can bind more strongly to the partially soft cobalt center of CoPc. The $-\Delta H^o_{BF_3}$ scale is based on BF_3, a very hard Lewis acid, which is expected to bind at the oxygen of DMSO; this discrepancy in coordination explains the enhanced response of CoPc sensors to DMSO. Isophorone (3,5,5-trimethyl-2-cyclohexene-1-one, 90.56 kJ·mol^{-1}) is unusual because it has a high reported $-\Delta H^o_{BF_3}$ value as compared to cyclohexanone (76.37 kJ·mol^{-1}). BF_3 has subsequently been shown to bind to alkenes with an enthalpy of 11.8 kJ·mol^{-1}, which may lead to overestimation of the $-\Delta H^o_{BF_3}$ value initially reported for isophorone.[52]

The sensor response follows a bilinear model, and an excellent least-squares fit (bilinear $R^2 = 0.952$) can be made by disregarding the two outliers discussed above. Including the outliers also gives a correlation (bilinear $R^2 = 0.738$) with a similar slope. By interpolation, relative basicity values can be predicted: water

(47) Lee, Y. L.; Tsai, W. C.; Maa, J. R. *Appl. Surf. Sci.* **2001**, *173*, 352−361.
(48) Chen, J. C.; Ju, Y. H.; Liu, C. J. *Sens. Actuators B* **1999**, *60*, 168−173.
(49) Kolesar, E. S.; Wiseman, T. M. *Anal. Chem.* **1989**, *61*, 2355−2361.
(50) Tongpool, R.; Yoriya, S. *Thin Solid Films* **2005**, *109*, 7878−7882.
(51) Atkins, P.; Jones, L. *Chemistry: Molecules, Matter, and Change*, 4th ed.; W. H. Freeman and Co.: New York, 2000.
(52) Herrebout, W. A.; van der Veken, B. J. *J. Am. Chem. Soc.* **1997**, *119*, 10446−10454.

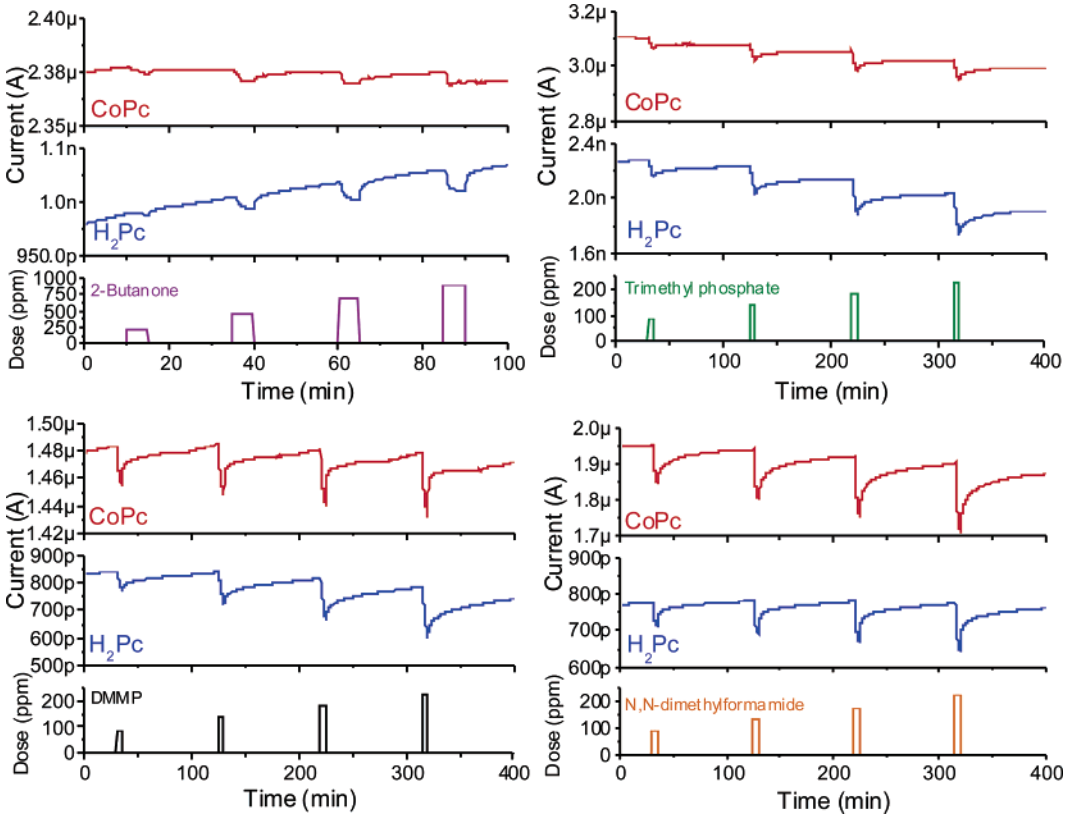

Figure 2. Sensor responses for CoPc (red) and H_2Pc (blue) to analytes 2-butanone (purple), trimethyl phosphate (green), DMMP (black), and DMF (orange). The top two traces in each graph represent the time-dependent current plots of the two sensors, while the bottom rectangular pulses in each represent the dosing of analyte as a function of time (i.e., valves to mix analyte into the flowing dry air stream are opened and closed).

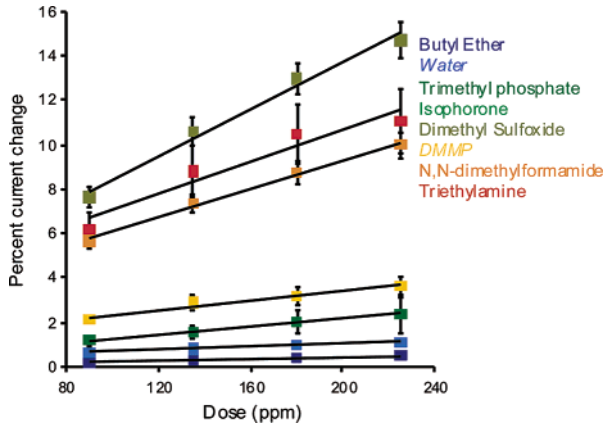

Figure 3. CoPc sensor response varies linearly with analyte concentration; slope R_C (% ppm^{-1}, $R^2 \geq 0.97$) for each may be used as a measure of sensor response. Some analytes have been omitted for clarity.

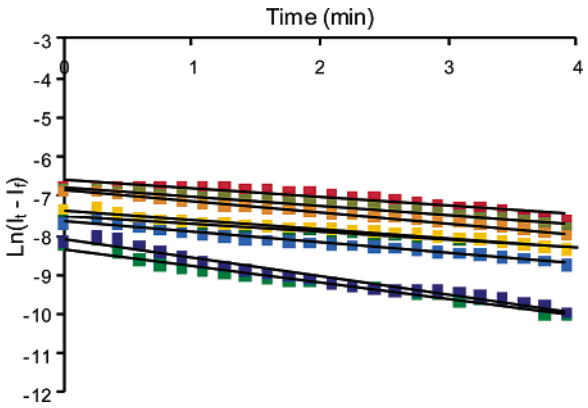

Figure 4. CoPc kinetics plots: $\ln(I_t - I_f)$ versus time is predominantly linear for all analytes, suggesting first-order kinetics.

$= 78.2$ kJ·mol^{-1} and DMMP $= 88.6$ kJ·mol^{-1}. We attribute this bilinear sensor response to competing physisorptive and chemisorptive effects.[53] Physisorption generally occurs for analyte absorption energies less than 40 kJ·mol^{-1}; above this threshold, chemisorptive processes occur.[49,54] Below the critical threshold, we propose that weak physisorption of analytes to the entire MPc molecular surface is occurring, which causes small resistance changes. Above the threshold, chemisorption at the metal and displacement of metal-bound O_2 are occurring, which provide the large resistance changes that correlate with analyte basicity. This is also supported by the fact that oxygen-dependent effects are only observed with analytes above the critical threshold and are strongest in the absence of O_2, while for analytes below this threshold, only rapid oxygen-independent sensor responses are seen even in the presence of O_2. These data show that the Lewis basicity of an analyte has a profound effect on the interaction between the analyte and the CoPc film. Comparison of sensor responses to bulk ligand parameters, such as vapor pressure and dipole moment, shows no such correlation (Figure 6).

4. H_2Pc Sensor Responses to Analytes. The H_2Pc sensors generally gave much lower currents. In contrast to CoPc, the H_2Pc R_C values do not correlate well with $-\Delta H^o_{BF_3}$, as can be seen in Figure 7A. However, the H_2Pc R_C values do correlate bilinearly ($R^2 = 0.905$) with analyte β_2^H (Figure 7B) with a

(53) Passard, M.; Pauly, A.; Blanc, J.-P.; Dogo, S.; Germain, J.-P.; Maleysson, C. *Thin Solid Films* **1994**, *237*, 272−276.
(54) Steed, J. W.; Atwood, J. L. *Supramolecular Chemistry*; J. Wiley & Sons, Ltd.: New York, 2000.

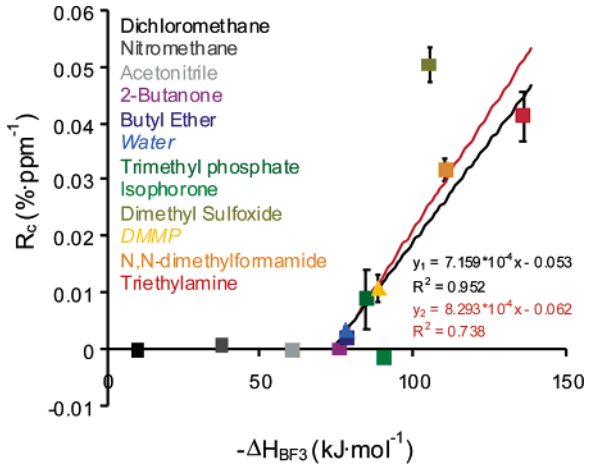

Figure 5. CoPc response slopes R_C versus $-\Delta H^o_{BF_3}$ for all analytes. Least-squares fits y_1 = neglecting outliers; y_2 = including outliers. Analytes represented by triangles have predicted $-\Delta H^o_{BF_3}$ values from the best fit line (y_1); error bars are present for all points.

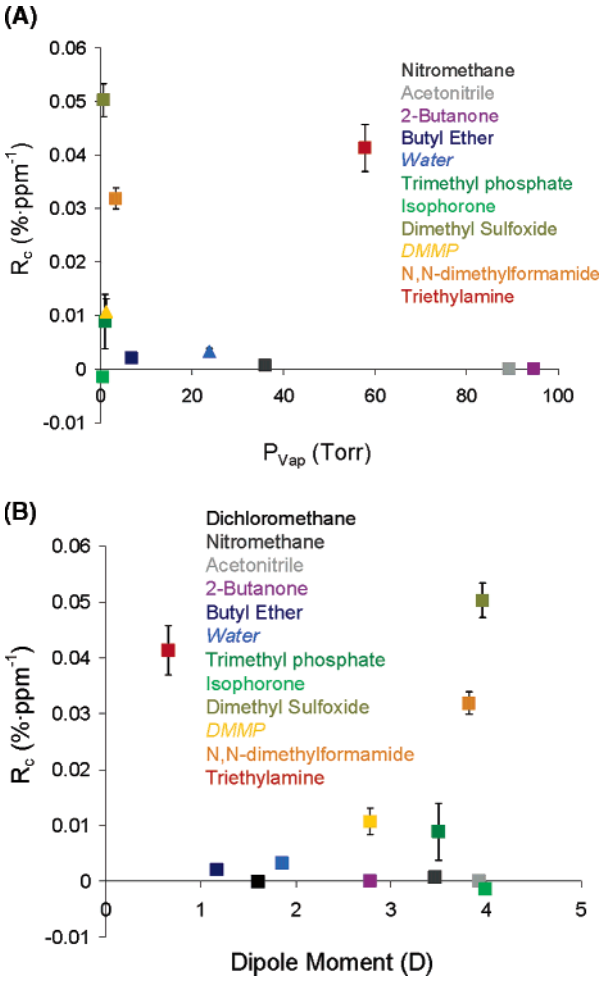

Figure 6. CoPc response slopes R_C as a function of (A) vapor pressure and (B) dipole moment, showing the lack of correlation.

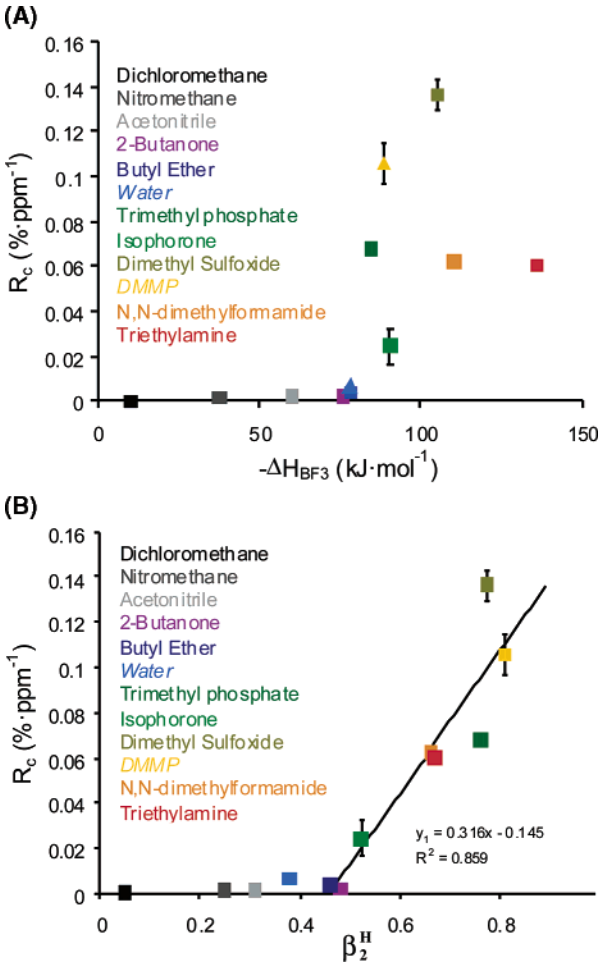

Figure 7. H_2Pc response slopes R_C as a function of (A) Lewis basicity $-\Delta H^o_{BF_3}$ and (B) hydrogen-bond basicity β_2^H. Error bars are less than the size of the data points in most cases.

Table 2. Sensor Responses and Appropriate Basicity Scales for Each Phthalocyanine and Analyte

analyte	$-\Delta H^o_{BF_3}$ (kJ·mol^{-1})	CoPc R_C (% ppm^{-1}) $\times 10^{-3}$	β_2^H	H_2Pc R_C (% ppm^{-1}) $\times 10^{-3}$
dichloromethane	10.0	-8.7×10^{-2}	0.05	0
nitromethane	37.63	0.6	0.25	1.5
acetonitrile	60.39	5.7×10^{-3}	0.31	1.7
2-butanone	76.07	3.7×10^{-2}	0.48	2.0
di-*n*-butyl ether	78.57	2.1	0.46	3.8
trimethyl phosphate	84.79	8.8	0.76	67.9
water		3.2	0.38	6.5
isophorone	90.56	−1.4	0.52	24.3
DMMP		10.7	0.81	105.7
DMSO	105.34	50.3	0.78	136.2
DMF	110.49	31.9	0.66	62.3
triethylamine	135.87	41.3	0.67	60.3

critical threshold of 0.46 units. This threshold behavior is again postulated to arise from a transition from physisorption to chemisorption as described above; however, chemisorption in this case arises from hydrogen bonding between analyte and the interior N−H hydrogens of H_2Pc molecules on the sensor film surface. In Table 2, the analyte values for both basicity scales are summarized along with the sensor responses of both Pcs next to the appropriate scale. The results of the CoPc and H_2Pc response studies lend support to a model that the molecular core is the primary source of chemical interaction in the Pc films for more strongly basic analytes. CoPc sensor response is dominated by analyte coordination chemistry, and H_2Pc is dominated by analyte hydrogen-bonding interactions. The presence of a critical threshold for this behavior may reflect when the entropic cost of specific ordered surface binding is offset by a favorable enthalpy of binding.

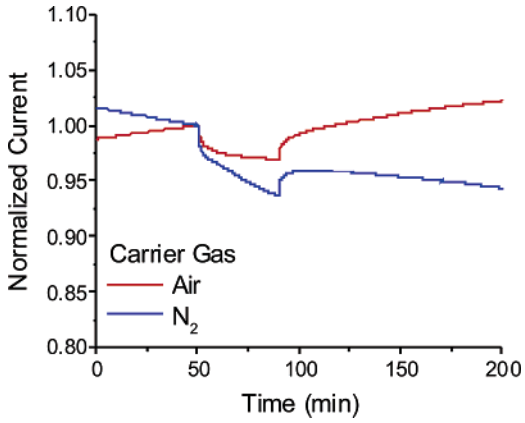

Figure 8. Normalized CoPc sensor responses to 225 ppm doses of water in UHP N_2 and zero grade air.

5. Oxygen Effects on Sensor Behavior. The influence of O_2 on the sensing behavior of the Pc films was explored by using either air or nitrogen as the carrier gas. According to the proposed model (vide supra), conductivity in Pc thin films arises by oxidation of the Pc film by O_2 (Scheme 1). The model gives two predictions for dosing in a nitrogen atmosphere: (a) before exposure to analyte, the nitrogen atmosphere will cause O_2 to gradually desorb from the film, decreasing the current; (b) upon exposure to analytes, analytes will displace residual O_2 irreversibly from the film, leading to incomplete recovery of current after dosing. The kinetically slower process of oxygen displacement makes these processes more important in longer exposure dosing. To test these hypotheses, CoPc and H_2Pc IDEs were dosed with 225 ppm of water for 40 min, with a recovery period of 180 min (18% duty cycle), using air as the carrier gas; this dosing was repeated using nitrogen. Figure 8 compares the time-dependent CoPc current plots for doses in both gases; H_2Pc behaves qualitatively similarly.

In this figure, several results can be seen. The sensor drift changes in the two different carrier gases; in nitrogen, the drift is -1.94% per hour, while in air, the drift is $+1.46\%$ per hour. This suggests that the film is gradually losing the dopant (and conductivity) when the carrier gas is O_2 free. There is also a stronger sensor response to water in nitrogen ($6.7 \pm 1.0\%$ CoPc, $6.65 \pm 1.9\%$ H_2Pc) than in air ($3.4 \pm 0.4\%$ CoPc, $2.6 \pm 1.4\%$ H_2Pc). These results can be attributed to reduced analyte$-O_2$ competition in the nitrogen atmosphere; the air dose still has O_2 present to compete with analyte for the binding sites, reducing the analyte effect on the film. Finally, in air, the sensor eventually completely recovers over time from the dose, but in nitrogen, the sensor never recovers completely (even over several days). In nitrogen, the fast component (C, Figure 1) is almost completely recovered, but the slower component (D, Figure 1) is not, suggesting that the slow effect arises from displacement of O_2. From a practical point of view, device operation is more stable and reproducible when operated in dry air. These results support the model that analytes both bind to free Pc sites and compete for O_2-bound Pc sites (Scheme 1).

Conclusion

The gas sensing behaviors of cobalt phthalocyanine (CoPc) and metal-free phthalocyanine (H_2Pc) thin films were investigated with respect to analyte basicity. There was a transition from physisorption to chemisorption once the analyte exceeded a critical basicity. It was found that the device response for CoPc increased significantly with analyte Lewis basicity, and for H_2Pc, sensor response increased significantly with analyte hydrogen-bond basicity. These results support the model that the analyte−phthalocyanine interaction is dominated by the central cavity of the phthalocyanine; coordination chemistry governs CoPc responses, and hydrogen-bonding interactions govern H_2Pc responses. The interactions of the two phthalocyanines with analytes were found to follow first-order kinetics. The influence of O_2 on the film response was examined, and it was found that competitive binding between analytes and O_2 significantly affects film response and recovery.

These films may be candidates for application as robust detectors. For example, EPA guidelines for exposure to Sarin gas (isopropyl methylphosphonofluoridate) list concentrations for disabling and lethal exposures; disabling exposures occur above 15 ppb for 10 min of exposure, while lethal exposures occur above 64 ppb for 10 min of exposure.[55] The responses reported above for DMMP detection suggest that with modest improvements in sensitivity they have potential to be used as part of a cross-reactive sensor array[56] or when interfaced with a micro gas chromatograph.[57]

Acknowledgment. The authors thank AFOSR for funding under MURI Grant #F49620-02-1-0288.

JA0689379

(55) National Research Council. *Acute Exposure Guideline Levels for Selected Airborne Chemicals*; The National Academies Press: Washington, DC, 2003; Vol. 3.
(56) Albert, K. J.; Lewis, N. S.; Schauer, C. L.; Sotzing, G. A.; Stitzel, S. E.; Vaid, T. P.; Walt, D. R. *Chem. Rev.* **2000**, *100*, 2595−2626.
(57) Lu, C. J.; Whiting, J.; Sacks, R. D.; Zellers, E. T. *Anal. Chem.* **2003**, *75*, 1400−1409.